Tissue electroporation

Observation of reversible electrical breakdown in viable frog skin

Kevin T. Powell, Ann W. Morgenthaler, and James C. Weaver
Harvard-M. I. T. Division of Health Sciences and Technology, Massachusetts Institute of Technology, Cambridge, Massachusetts 02139

ABSTRACT Experiments by others have used isolated cell or bilayer membrane preparations to study the dramatic phenomena associated with electroporation. The present study observes electroporation behavior in an intact tissue. Viable samples of frog skin (*Rana pipiens*) were exposed to short electrical pulses of varying width and magnitude under "charge injection" conditions. After a pulse, the transtissue potential decayed with two distinct time constants, one short ($\tau_s \approx 0.3$ ms) and the other longer ($\tau_L \approx 2$ ms). Above thresholds for the pulse magnitude and for the pulse width τ_L decreased significantly, with progressively smaller τ_L as the pulse magnitude and width increased. The postpulse potential, $\Delta U_{tissue}(t)$, and resistance, R_{tissue}, also decreased progressively. The tissue subsequently recovered to its original resistance and open circuit potential, $\Delta U_{tissue,oc}$, within 2–3 min after a pulse. At that time another pulse experiment could be carried out, demonstrating repeatability and reversibility. No significant permanent changes in R_{tissue} and $\Delta U_{tissue,oc}$ were found. This is interpreted as avoidance of significant tissue damage. Taken together, these dramatic phenomena are characteristic of the reversible electrical breakdown previously observed in charge injection experiments with artificial planar bilayer membranes and with isolated cell membranes by similar very short pulses. The present experiments therefore demonstrate that electroporation can be repeatedly caused and observed in a viable tissue without apparent damage.

INTRODUCTION

"Electroporation" is used here to denote the occurrence of significant openings or pores in bilayer membranes due to elevated transmembrane potentials, and is now believed to be a universal phenomenon for artificial bilayer and cell membranes (Neumann et al., 1989; Zimmermann, 1986). One dramatic manifestation of electroporation is reversible electrical breakdown (REB), which is a very rapid electrical discharge of the transmembrane potential, followed by recovery of a membrane to its initial resistance (Stämpfi, 1958; Zimmermann et al, 1973; Coster and Zimmermann, 1975; Benz et al., 1979; Benz and Zimmermann, 1980*a* and *b*, 1981; Chernomordik et al., 1982, 1983, 1987; Sukharev and Chizmadshev, 1982; Glaser et al., 1988). In striking contrast, imposition of smaller transmembrane potentials for longer times generally does not cause REB, but instead leads to a nonthermal rupture in planar bilayer membranes (Crowley, 1973; Abidor et al., 1979; Benz et al., 1979). It is presently believed that either REB or rupture can occur in individual planar bilayer membranes by varying only the applied electrical stimulus (Benz et al., 1979; Powell et al., 1986; Barnett, A., and J. C. Weaver, submitted for publication). As described in studies cited above, experiments of others have amply demonstrated REB in planar artificial bilayer membranes and in the membranes of isolated cells. In the much more complex system of cells which comprises tissue, recent evidence suggests that electroporation is the cause of nonthermal damage associated with electrocution injury, as experiments show large, permanent changes in muscle tissue resistance after large electrical pulse stimulus (Lee et al., 1988). However electroporation may not be the proximate cause of damage. Instead cell lysis may be a consequence of a long-lived high-permeability state of electroporated cell membranes, resulting in exchange of molecules and ions between intracellular and extracellular volumes, leading to chemical imbalances with cause cell lysis (Kinosita and Tsong, 1977; Weaver et al., 1988; Michel et al., 1988).

As the term "electroporation" suggests, transient pores are widely believed to be involved in REB. For example, it has been shown that the occurrence of REB and rupture in planar bilayers can be explicitly and quantitatively described using physical descriptions of water-containing pores. Specifically, the magnitude and temporal behavior of the transmembrane potential and membrane resistance can be correctly described by a theory based on a distribution of transient aqueous pores which vary significantly in both size and number (Powell et al., 1986; Weaver and Powell, 1989; Barnett, A., and J. C. Weaver, submitted for publication). REB is of interest because it provides a readily measured indication of the occurrence of the dramatic phenomenon of electroporation.

Address correspondence to James C. Weaver

0006-3495/89/12/1163/09 $2.00

One class of previous experiments directed towards a detailed study of REB characteristics has involved "charge injection" protocols. In these studies very short pulses in the range of 0.1 to 100 μs were applied, and the transmembrane potential was allowed to decay through the time-dependent membrane resistance (Benz et al, 1979; Benz and Zimmermann, 1980*a* and *b*, 1981). Another class of studies ("voltage clamp") involved a wider range of pulse durations, and often emphasized longer pulses, but constrained or clamped the transmembrane potential and then measured the resulting transmembrane current, $I(t)$ (Abidor et al., 1979; Chernomordik et al., 1983, 1987; Glaser et al., 1988). Although key features differ, dramatic behavior is observed in all of these studies. We used a charge injection protocol and compared our results to the corresponding cell membrane and artificial bilayer studies.

More specifically, the present study used pulses in the range of 10 to 100 μs, so that it is relevant to summarize the key features of REB previously observed in cell and planar membranes using similar short pulses. (*a*) These previous experiments were conducted with pulse widths ranging from ~0.1 to ~100 μs. (*b*) At fixed pulse width, as the pulse magnitude was increased the sample's resistance remained essentially unchanged for small pulses. However, for pulses above some threshold the resistance decreased dramatically. Artificial bilayer membranes, with a very large initial resistance (e.g., 10^9 ohm), exhibited temporary resistance decreases of seven to eight orders of magnitude within several hundred nanoseconds. Cells, which have much smaller initial membrane resistance, exhibited smaller fractional changes. After the pulse the transmembrane potential, $U(t)$, decayed almost exponentially, with an approximate RC time constant governed by an essentially unchanged membrane capacitance, C, but a greatly decreased membrane resistance, R. In fact, not only did $R(t)$ decrease dramatically, it continued to change throughout both the breakdown and recovery phases. Above an approximate threshold, still larger values of U resulted in even lower resistances. (*c*) After reversible electrical breakdown, the resistance recovered to its initial value with recovery times ranging from microseconds (artificial planar bilayers) to seconds or even minutes (cell membranes). Such reversibility allowed repeated experiments to be carried out with the same membrane. (*d*) If REB occurred, the destructive phenomenon of rupture (irreversible electrical breakdown) of planar bilayer membranes was generally avoided, even though longer pulses of smaller magnitude usually caused rupture (Crowley, 1973; Abidor et al., 1979; Benz et al., 1979; Weaver and Mintzer, 1981; Sugar, 1981). The evidence to date suggests that whereas rupture is clearly an irreversible and damaging phenomenon, REB itself is not directly associated with cellular or membrane damage. This is an impressive notion, because typical transmembrane potentials, $U(t)$, associated with REB caused by very short pulses are in the range of $-500 < U < 1{,}500$ mV. These values are well above cellular resting potentials of $-50 < U < 150$ mV, and also generally above the range of transmembrane potentials of $-200 < U < 500$ mV, which cause destructive rupture in planar bilayer membranes.

Although these artificial planar bilayer experiments have provided a significant amount of data, there are only a small number of previous studies which have directly measured electrical behavior during and/or after REB in cell membranes. In fact, most electroporation studies of cells have not directly measured electrical parameters such as $U(t)$ at the cellular level. Instead they have focused on uptake or release of molecules and of radioactive ions, and on biological endpoints such as transfection (Neumann et al., 1989; Zimmermann, 1986). The small number of experiments involving direct electrical measurements have included measurements of the time-dependent transmembrane potential, $U(t)$, in the frog nerve (Stämpfi, 1958), algal cells (Benz and Zimmermann, 1980*a*), squid axon (Benz and Conti, 1981), and also measurements of the time-dependent transmembrane current $I(t)$ in membranes of the human erythrocyte and of L cells (Chernomordik et al., 1987). Taken together, these previous cell membrane and artificial planar membrane observations are important for comparison to the occurrence of REB in tissue.

APPARATUS AND METHODS

A simple Lucite double chamber was used (Fig. 1), which is similar to designs of others (Helman and Miller, 1971; Helman and Fisher, 1977). Each chamber was filled with ~50 ml of Ringer's (chloride) solution (5.8 g/liter NaCl, 0.15 g/liter KCl, 0.29 g/liter $CaCl_2 \cdot 2H_2O$, 0.20 g/liter $NaHCO_3$, and 2.0 g/liter glucose). The tissue area exposed to Ringer's solution was $A_{tissue} \approx 1.3$ cm^2. Four electrodes consisting of two separate sense electrodes and pulse application electrodes were used. Each application electrode consisted of a perforated stainless steel sheet, with an estimated effective surface area of ~8 cm^2. The perforations allowed the electrodes to be placed within a few millimeters of the skin while still allowing diffusion of nutrients and metabolites to and from the skin. The large electrode effective area allows the surface current density to be low, reducing the potential drop at application electrodes (Geddes, 1972). This allows more of the measured application potential to appear across the tissue. Large electrodes also assured that a uniform electric field was applied to the tissue. The sense electrodes consisted of either calomel or $Ag^+/AgCl$ electrodes connected to the chambers by a ceramic junction (model 13-639-79 or 13-639-53, Fisher Scientific Co., Pittsburgh, PA). The sense electrodes were located behind the application electrodes in each of the two chambers. The sense electrodes were allowed to equilibrate in 4 M KCl for 2–3 d before use, then giving a junction potential of <0.5 mV.

The overall circuit schematic (Fig. 2) was designed to allow application of either current ramps or voltage pulses (0–30 volt amplitude square wave) to the skin. The current ramp generator had adjustable

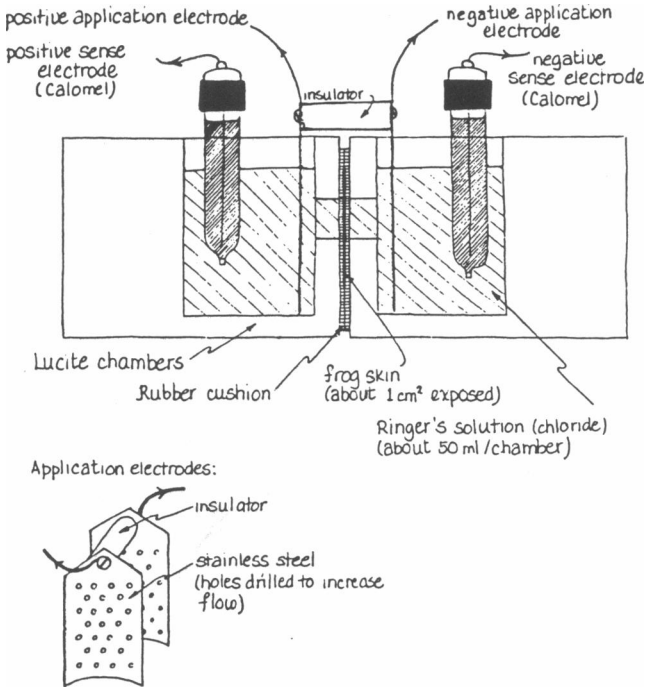

FIGURE 1 Drawing of the experimental apparatus. Viable frog skin with ~1.3 cm^2 of exposed tissue was clamped between the two chambers, with a rubber gasket or cushion providing a seal without the need for extensive crushing of the clamped tissue. Each chamber contained ~50 ml of Ringer's solution. Two sets of electrodes were used: a pair of stainless steel current application electrodes (*bottom*), and a pair of calomel measurement or sense electrodes for transtissue potential measurement.

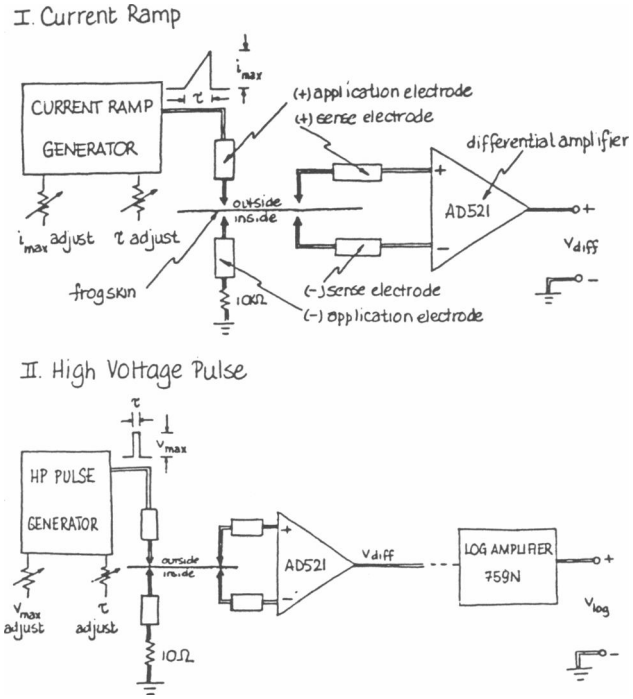

FIGURE 2 Schematics of circuits used in the application of currents and potentials, and in the acquisition of transtissue electrical signals. (*I*) The current ramp generator, showing the sites of the current application electrodes with respect to the inside and outside surfaces of the frog skin when in the chamber. (*II*) High voltage pulse generator circuit, which consists of a Hewlett-Packard model 214A pulse generator (Hewlett-Packard Co., Palo Alto, CA) connected as shown with respect to the inside and outside surfaces of the frog skin.

sweep (period τ), baseline, and maximum current settings. Once set, the current ramp baseline had negligible drift. Transtissue currents during use of the low-level current ramp runs were monitored by developing a potential drop across a precision 10K resistor. The voltage pulse generator (model 214A, Hewlett-Packard Co., Palo Alto, CA) had a nominal output impedance of 50 ohm for pulses of 0–30 V. For both current ramps and voltage pulses the differential potential across the skin was measured using a high-impedance (10^9 ohm) differential amplifier (model AD521, Analog Devices, Inc., Norwood, MA) with an input bias current of 80 nA. The output of the differential amplifier could be displayed directly on a fast storage oscilloscope (model 7A26/7623A, Tektronix, Inc., Beaverton, OR) and then photographed (C-5C camera, Tektronix, Inc.). Alternatively, the output of the AD521 was directed to a logarithmic amplifier (model AD759N, Analog Devices, Inc.), which expanded and linearized the exponentially decaying transtissue voltage after a pulse. The logarithmic amplifier provided a useful dynamic range of three decades of voltage input (10 mV to 10 V), which was sufficient for the signal range of interest. The maximum error was estimated to be 1% over the range 10 mV to 2 V. This output was also displayed on the oscilloscope and photographed. Manual digitization of photograph tracings allowed subsequent computer analysis.

In vitro preparations of viable frog skin (*Rana pipiens*) were selected as a model tissue for two reasons: (*a*) a significant literature on the properties of isolated frog skin, including its electrical properties, and (*b*) ease of manipulation and ready sources of supply. Electrical parameters which afford convenient measurement of the condition of frog skin include the open circuit potential $\Delta U_{tissue,oc}$, the short circuit current I_{sc}, and the transtissue resistance, R_{tissue} (Helman and Miller, 1971, 1977). The resting potential $\Delta U_{tissue,oc}$ (typically −30 mV) is maintained by active transport of Na^+ and K^+ across the skin. The short circuit current I_{sc} is readily measured by forcing both sides of the skin to the same potential, i.e., a voltage clamp condition, and measuring the resulting current across the skin. The transtissue resistance, R_{tissue}, can be measured straightforwardly. Any significant reduction in transtissue resistance, or damage to the cells responsible for the active transport, should be reflected in $\Delta U_{tissue,oc}$ and I_{sc}.

Frogs were sacrificed by pithing, and a 4–6-cm^2 piece of abdominal skin was excised and placed between the chamber halves under gentle pressure. The perimeter of the skin was coated lightly with silicone grease (Dow Corning Corp., Midland, MI) to obtain a better seal. The skin was allowed to equilibrate while bathed with Ringer's for 30–120 min before measurements were taken. The temperature was 25 ± 2°C. Depolarizing potentials or currents were used throughout, i.e., positive current was passed from the serosal (outside, spontaneously negative) to the mucosal (inside, spontaneously positive) surface of the skin. Current ramps were initially used at low levels to determine $\Delta U_{tissue,oc}$, I_{sc}, and R_{tissue} at the beginning of a set of experimental runs. As reported by others (Finkelstein, 1964; Candia, 1970; Helman and Miller, 1971, 1977), both $\Delta U_{tissue,oc}$ and I_{sc} gradually decreased with time during control periods when no large ramps or voltage pulses were applied. This decrease is interpreted by us as a gradual deterioration of the metabolic

activity and viability of the tissue and represents a normal experimental condition. Typical initial values were:

Short circuit current density	J_{sc}	= 20–60 μA/cm^2
Open circuit potential	$\Delta U_{tissue,oc}$	= −10 to −95 mV
Specific transtissue resistance	R_{tissue}	= 800–1,500 ohm cm^2.

These values are consistent with those in the literature cited above. The range of values from skin to skin is also consistent with the variability found by others. Because of this interskin variability, however, comparison of skin parameters from different skin preparations is not warranted.

RESULTS AND DISCUSSION

Current ramps and voltage pulses were applied repeatedly to each frog skin sample, beginning with high level current ramps in several early experiments (Fig. 3). These experiments demonstrated the occurrence of an action potential above a threshold current, which is consistent with previous observations of others (Finkelstein, 1964; Candia, 1970). Our use of high-level current ramps served mainly to verify that we could reproduce the results of these previous investigations, where (at still higher currents) a sudden decrease in slope was observed.

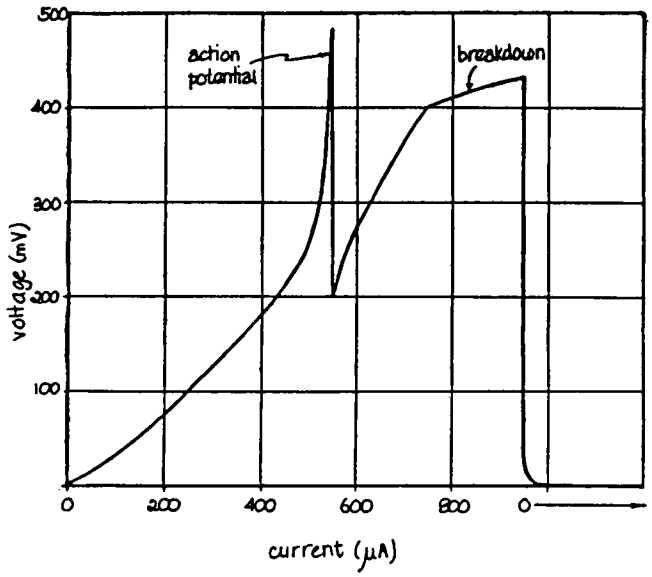

FIGURE 3 Plot of the transtissue potential ("voltage") as a function of the applied current for an overly large current ramp, an atypical case. The applied current ramp results in an approximately linear rise in voltage until ~500 μA, at which point an action potential is triggered. Upon applying still larger currents the tissue undergoes some type of breakdown (slope change corresponding to a decrease in transtissue resistance) at ~750 μA, and at ~950 μA the current ramp is terminated. This type of experiment by itself does not adequately reveal whether or not REB has occurred.

This sudden change in tissue resistance is termed "breakdown" in the literature. In the present study, a refractory period was observed upon repetition of the current ramp within 30–60 s, during which no action potential was observed. However, the sudden slope decrement at higher currents was still observed. Although it is tempting to identify this slope change with REB, such an interpretation cannot be made with certainty from this type of data.

It is clear in the present work, however, that the use of voltage pulses in a charge injection protocol can cause REB in frog skin (Figs. 4 and 5), and that key features of the reversible breakdown are similar to those observed in artificial bilayer membranes and in isolated cells using charge injection. In our experiments voltage pulses of 1–100 μs width and 1–20 V amplitude at the generator output terminals were applied to the chamber. As is the case with planar bilayer membrane measurements (Benz et al., 1979), most of the potential drop occurred across the application electrodes and within the electrolyte (Ringer's solution) between the electrodes and the skin.

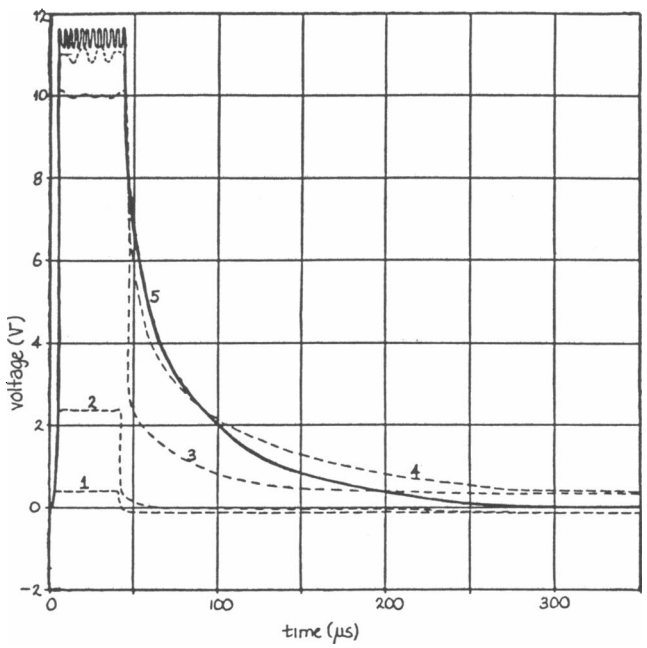

FIGURE 4 Tracings of transtissue potentials (voltage) during and after the application of a constant pulse (width ≈ 50 μs). Five different transtissue pulses are shown, with *1–4* drawn as dashed lines and *5* drawn as a solid line: (*1*) 1 V; (*2*) 2 V; (*3*) 5 V; (*4*) 10 V, (*5*) 20 V. Tracing *5* crosses curve *4* at ~80 μs and curve *3* at ~200 μs, and curve *4* crosses curve *3* at $t > 350$ μs. This behavior, characteristic of reversible electrical breakdown (REB), is interpreted as due to a significantly smaller transtissue resistance caused by electroporation (Powell et al., 1986; Weaver and Powell, 1989; Barnett, A., and J. C. Weaver, submitted for publication), and is taken here as evidence of the occurrence of REB.

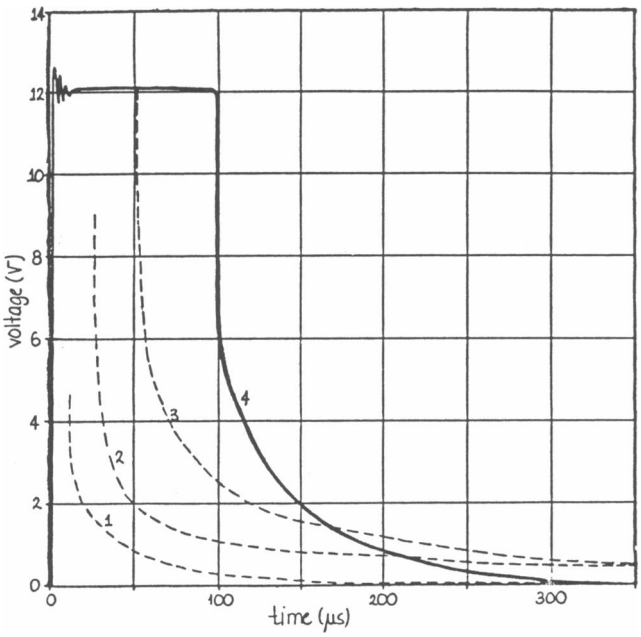

FIGURE 5 Tracings of transtissue potentials (voltage) during and after the application of 10-V pulses of different pulse widths. Four different pulses are shown, with *1–3* drawn as dashed lines and *4* drawn as a solid line: (*1*) 10 μs; (*2*) 30 μs; (*3*) 50 μs; (*4*) 100 μs. Tracing *4* crosses curve *3* at ~165 μs, and curve *2* at ~215 μs. This behavior is also characteristic of REB.

For this reason it was not possible to make useful measurements during the application of pulses. Instead, and as in previous bilayer membrane experiments, measurements were made immediately after the pulse ceased, so that electrode and bathing electrolyte potential drops were negligible. The maximum transtissue potential was then found to be ~1.5 V. From this we infer that the transmembrane potential of the cells comprising frog skin (essentially a monolayer of cells connected by tight junctions) was ~750 mV, in approximate agreement with previous observations of others using isolated cells and artificial planar bilayer membranes. An interval of 2 or 3 min between pulses was used to allow for recovery of the skin after any breakdown that might have occurred.

Both the pulse width Δt and pulse amplitude ΔU_i were varied to test behavior in the Δt-ΔU_i plane (see Tables 1–3). The order in which Δt-ΔU_i pairs were tried was randomized. In our experiments the decay of the transtissue potential was of primary interest, and was dominated by the long time constant τ_L in the time interval of 1–5 ms after a pulse. Each pulse decay was observed on the storage oscilloscope and photographed. Both linear and logarithmic displays were used. Linear displays provided a qualitative estimate of the occurrence of REB, whereas the logarithmic displays allowed more accurate quantitative assessment of the occurrence of REB. The decaying potentials were measured, manually digitized, and then analyzed on a computer to determine the long and short time constants, τ_L and τ_S. Specifically, the decaying potentials were fit to the equation

$$\Delta U_{tissue}(t) = \Delta U_{tissue,S}e^{(-t/\tau_S)} + \Delta U_{tissue,L}e^{(-t/\tau_L)} + \Delta U_{tissue,baseline}, \quad (1)$$

where $\Delta U_{tissue,S}$, $\Delta U_{tissue,L}$, and $\Delta U_{tissue,baseline}$ are constants obtained from the fit.

Fig. 4 shows an example of a linear plot of several

TABLE 1 Comparison of observed variation in long time constant (τ_L) for combinations of pulse amplitude (ΔU_i) and pulse width (Δt) for single preparation of frog skin

	Pulse amplitude ΔU_i			
Pulse width Δt	2 V	5 V	10 V	20 V
μs	*ms*	*ms*	*ms*	*ms*
10	*	1.9	2.0	1.8
20	*	1.9	1.9	1.5
50	1.9	1.9	1.6	1.2
100	2.0	1.6	1.3	1.3

Upper left region within the table is associated with prebreakdown values, whereas region to the lower right has shorter time constants, and these are interpreted by us as corresponding to reversible electrical breakdown, the electrical signature of electroporation. Unlike previous experiments with individual cells or artificial planar bilayer membranes, these tissue measurements involve a large number (of order 10^6) of cells, so that some averaging or smoothing of the individual cell REB behavior is expected. Nevertheless, a distinct threshold region is observed, suggesting that either most cells experience REB for about the same pulse parameters, and/or that the tissue electrical behavior is dominated by the cells with the lower thresholds. *Small pulses had corresponding transtissue potentials which were too small to accurately determine τ_L.

TABLE 2 Decay time constant (τ_L) for various combinations of pulse amplitude (V) and pulse width (μs) for a different frog skin preparation

	Pulse amplitude ΔU_i			
Pulse width Δt	2 V	5 V	10 V	20 V
μs	*ms*	*ms*	*ms*	*ms*
10	6.4	6.2	3.1	2.8
20	5.4	5.0	3.6	2.1
50	5.2	2.7	2.6	2.2
100	3.2	2.5	1.6	1.7

Region to upper left of the solid line boundary is associated with prebreakdown values, whereas the region to lower right has progressively shorter time constants, and these are interpreted by us as corresponding to reversible electrical breakdown, the electrical signature of electroporation. Again, the broad transition rather than a sharp threshold is consistent with the involvement of a large number of cells.

TABLE 3 Extrapolated transtissue potential ($\Delta U_{tissue,0}$) for various combinations of pulse amplitude (V) and pulse width (μs) for single frog skin preparation

	Transtissue potential at pulse end, $\Delta U_{tissue,0}$			
Pulse width Δt	2 V	5 V	10 V	20 V
μs	*ms*	*ms*	*ms*	*ms*
10	0.03	0.14	0.30	0.74
20	0.08	0.22	0.57	1.28
50	0.14	0.50	1.32	0.89
100	0.34	1.48	0.85	0.74

This extrapolated potential is obtained by performing a logarithmic extrapolation of the decaying potential, but using only the portion of the curve dominated by the long time constant, τ_L. The extrapolated values of $\Delta U_{tissue,0}$ have a maximum value of ~1,500 mV, consistent with the interpretation that the basal monolayer of cells in the hydrated frog skin experiences electroporation when the transmembrane potential reaches ~750 mV. Pulses which would otherwise give larger transtissue values cause electroporation, such that the potential decays during the applied pulse produce smaller values of $\Delta U_{tissue,0}$ (the lower right three entries). This is consistent with observations of reversible electrical breakdown of artificial planar bilayer membranes and isolated cells caused by pulses of similar duration using a charge injection protocol (Benz et al., 1979; Benz and Zimmermann, 1980*a* and *b*).

superposed responses of a tissue to pulses of constant width and increasing amplitude. A characteristic feature of REB is evident: at higher pulse amplitudes the decay becomes noticeably faster. An example of a similar linear plot is given in Fig. 5, wherein the pulse amplitude is fixed and the pulse width is increased. This reveals the same characteristic of REB: once a voltage threshold is reached, an increased pulse width results in progressively more rapid exponential decay after the pulse has ceased. This is a key finding of the present study, as it shows that the same immediate postpulse behavior is observed in this tissue as has been previously found in short-pulse experiments on cell membranes and artificial planar bilayer membranes. The basic striking features are present, even though this tissue consists of a large number of cells, which would be expected to cause averaging, and therefore smoothing, of the individual cellular REB behavior.

For a more comprehensive examination of the tissue response to pulses of varying amplitude and width, a two-dimensional representation based on pulse amplitude (ΔU_i) and pulse width (Δt) is useful. A convenient tabulation of the results from any individual frog skin is a grid wherein $\Delta U_{tissue,O}$ and τ_L are shown for different values of the pulse width Δt and pulse amplitude ΔU_i (Tables 1–3). The use of a charge injection protocol implies that the pulse durations are much shorter than the decay times after the pulse, and that the key independent variable is actually the injected charge, Q, which accumulates across the capacitance of the tissue, C_{tissue} (Barnett, A., and J. C. Weaver, submitted for publication). However, to compare our results with the previous REB studies on artificial planar bilayers and on isolated cells, we used ΔU_i and Δt as independent variables, as was done in those previous charge injection studies by others. Not surprisingly, the particular value of τ_L at the same ΔU_i and Δt does vary between different tissues. Of considerable significance is the presence of a region (the lower right) in each of the tables wherein significantly smaller values of τ_L are found. The existence of this lower right region is consistent with a smoothed threshold for REB, as might be expected due to the large number (10^6) of cells. We interpret this as the occurrence of REB in tissue. As in the case with experiments on artificial bilayers and on isolated cells, the transtissue potential at the end of a pulse, $\Delta U_{tissue,O}$, also can indicate the occurrence of REB. Specifically, $\Delta U_{tissue,O}$ reaches a maximum, and then decreases in cases where τ_L has also markedly decreased. For cases without breakdown, $\Delta U_{tissue,O}$ behaves approximately like the potential of a capacitor (the tissue) which is charged by the voltage pulse. However, if the potential exceeds ~1,500 mV (equal to that found for one or two isolated cell transmembrane potentials at breakdown), then the behavior changes markedly. Reversible electrical breakdown occurs, τ_L drops, and $\Delta U_{tissue,O}$ decreases compared to subbreakdown values.

As a test for permanent changes indicative of tissue damage, low-level current ramps were used at the beginning, midpoint, and end of the voltage pulse runs. These current ramps gave values of $\Delta U_{tissue,oc}$, I_{sc}, and R_{tissue}. We expected gradual decreases (as found in control intervals) to be normal. Had any sudden decreases in these parameters occurred, they would have presumably reflected the occurrence of damage. However, no sudden decreases were observed.

We can estimate the degree of one type of damage as follows. If even a small fraction of the cells in a macroscopic tissue is damaged to the point of lysis, a permanent, measurable reduction in the transtissue resistance, R_{tissue}, would be expected. Specifically, if the fractional resolution of the R_{tissue} measurement is $X \equiv \delta R_{tissue,RMS}/R_{tissue}$, the absence of a measurable change within experimental error can be converted into an estimate of the number of lysed cells, $N_{cells\ lysed}$, which open to form cell-size holes across the tissue. More specifically, an upper bound on $N_{cells\ lysed}$ is estimated simply by using a "signal-to-noise" ratio of one as a criterion. That is, we set $\delta R_{tissue,RMS}$ ("noise") equal to $\approx \Delta R_{tissue}$ ("signal"), where the change, ΔR_{tissue}, is the initial transtissue resistance, $\Delta R_{tissue,i}$, minus the resistance of the tissue containing $N_{cells\ lysed}$ cell-size holes. A typical cell in frog skin *Stratum corneum* has a thickness of $w \approx 5$ μm and an area of $A_{cell} \approx 50$ μm^2 (Berridge and Oschman, 1972), so that the resistance of a hole of this size filled with Ringer's chloride of resistivity $\rho_{saline} \approx 100$ ohm cm is about $R_{hole} = \rho_{saline} w/A_{cell} \approx 10^5$

ohm. We found that viable frog skin had a specific area resistance of $\sim 10^3$ ohm cm^2, so that the area of 1.3 cm^2 had a resistance of 800 ohm. Frog skin contains $\sim 2 \times 10^6$ cells/cm^2, so that one cell has a transcellular resistance of about $R_{cell} \approx 2 \times 10^9$ ohm $\gg R_{hole}$. Thus, the value of R_{tissue} after the appearance of a $N_{cells\ lysed}$ holes can be approximated by the parallel combination of the initial value of R_{tissue} and $N_{cells\ lysed}$ resistors of magnitude R_{hole} connected in parallel, which yields the estimate,

$$N_{cells\ lysed} \approx \frac{X R_{hole}}{R_{tissue,i}}. \quad (2)$$

In our experiments no measurable permanent decrease in R_{tissue} was found. Instead, only temporary decreases were observed, and these were fully reversible within experimental measurement error. The resolution of the R_{tissue} measurement was 3% or better, (i.e., $X \leq 3 \times 10^{-2}$). This leads to the estimate that $N_{cells\ lysed} \approx 4$ lysed cells could be detected in the presence of $\sim 3 \times 10^6$ cells in the tissue preparation, i.e., a cell lysis fraction of order 10^{-6}. In several experiments, 20 or more pulses of varying magnitude and width were used to cause electroporation in the same tissue preparation, and yet the overall observed change in R_T due to these multiple pulses was less than the measurement resolution of 3%. Although multiple pulse behavior was not a primary objective of these experiments, these results suggest that a fractional cell lysis rate per pulse was less than $\sim 10^{-7}$ per pulse, i.e., that fewer than one cell in 10^7 cells was lysed for each pulse. For these reasons, our interpretation of these experiments is that reversible and nondamaging electroporation phenomena have been observed in an isolated viable tissue.

The measurement of R_{tissue} alone does not, however, provide a measure of more subtle damage which may lead to delayed cell death (Kinosita and Tsong, 1977; Weaver et al., 1988; Michel et al., 1988), and which may be responsible for the significant permanent damage observed in intact muscle preparations (Lee et al., 1988). Although it has not been carefully investigated here, it is plausible that the ability of isolated viable frog skin to generate quasi-steady-state potentials and currents through metabolic activity provides a more stringent test of damage. If there were a significant number and size of persistent residual pores after the membrane recovery phase of electroporation, these pores would be expected to provide significant shunt pathways for the ubiquitous small ions such as Na^+, K^+, and Cl^-, and should be reflected promptly in a decrease in the tissue potential or current. However, we also found no significant changes in $\Delta U_{tissue,oc}$ or I_{sc} beyond the normal downward drift over several hours which occurs as the tissue slowly deteriorates, and its metabolic activity gradually diminishes. Therefore our results are consistent with the interpretation that tissue electroporation has occurred, as reversible electrical breakdown occurs without apparent damage to the tissue, even with repeated pulse applications.

The final test for reversibility consisted of a series of low-level current ramps, before and after a voltage pulse, to determine the kinetics of recovery. The time dependence of the recovery of the tissue (after pulse experiments with either increasing ΔU_i or Δt) was monitored by using low-level current ramps (Candia, 1970). The oscilloscope was set to such a slow sweep that the ramp appears as a nearly vertical line (Fig. 6). The difference between the top and bottom of the "envelope" of these successive current ramps (fixed excurison in I) is a direct measure of the tissue resistance. Simple inspection of Fig. 6 shows qualitatively that there is a rapid recovery after application of a single pulse (width not discernible on the time scale of Fig. 6). Whereas there is some moderately complicated structure to the envelope, inspection shows that most of the recovery occurs within ~ 20 s after a pulse. Over a longer period (~ 2–3 min) the

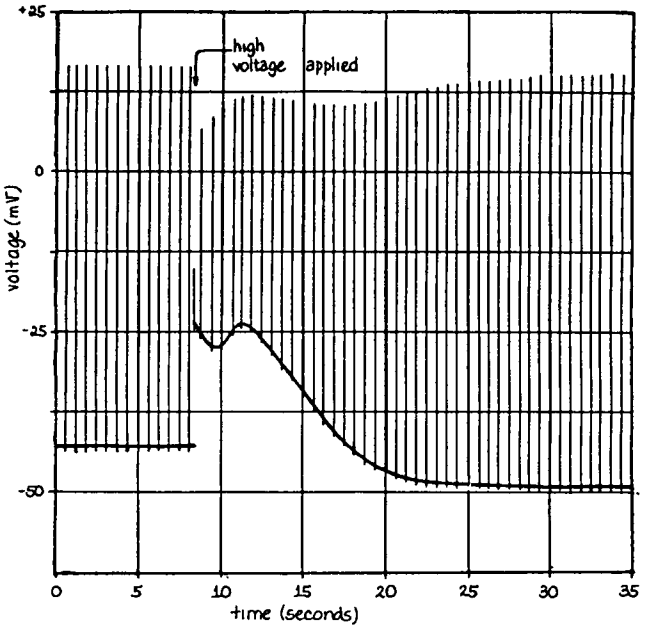

FIGURE 6 Observation of the reversible nature of the breakdown, as revealed by the recovery of the transtissue potential after the application of a pulse which causes REB. The time scale is significantly different than in Figs. 4 and 5, so that a succession of evenly applied current ramps appears here as a train of evenly spaced spikes. Before the pulse (arrow denoting "high voltage") the spikes are of constant size. Immediately after the single pulse, the magnitude of the spikes decreases to about one-half the prepulse value, and then recovers over a time of ~ 20 s. Both the top and the bottom of the spikes initially change, presumably because the open circuit potential developed by the frog skin tissue is perturbed, and both the applied current related potential drop and the open circuit potential contribute to the measured transtissue potential.

recovery appears essentially complete. The ability to repeatedly observe this essentially complete recovery is also a key feature of these experiments, reflecting the reversibility of the electrical breakdown due to electroporation.

The extension of reversible electrical breakdown measurements from artificial bilayer or isolated cell membranes to tissue can give some insight into electroporation effects in a tissue, and may be particularly useful as a readily measured indicator of electroporation. The macroscopic viable tissue preparation provides a convenient system for detecting the presence of any prompt major damage due to electroporation. Further, electrical monitoring for major damage is convenient and reasonably stringent.

Given the absence of measurable damage, the observation of behavior characteristics of REB is significant. After a pulse the passive response of the skin appears to be adequately described by two series RC circuits, with two corresponding time constants, τ_S and τ_L. As shown here, reversible electrical breakdown was repeatedly demonstrated in samples of isolated viable frog skin. Overall, after several applications of pulses of different magnitude and width causing REB, there is no evidence of damage, as the electrical parameters of transtissue resistance, short circuit current, and open circuit potential all rapidly return (within experimental resolution) to their initial values.

In summary, experiments carried out on preparations of viable frog skin demonstrate that electroporation can be made to occur repeatedly in a tissue, without apparent damage. Reversible electrical breakdown, which is one consequence of electroporation, under charge injection conditions results in characteristic decay behavior. Above an approximate threshold for either applied potential amplitude or pulse width, progressively more rapid decays are observed, in agreement with previous studies by others on artificial bilayer membranes or on cell membranes. Within 2–3 min after pulse application the transtissue resistance recovered completely, as did the open circuit potential developed by the tissue. Multiple pulses, separated by 2–3 min, could be repeatedly applied, and no permanent changes in transtissue resistance or open circuit potential were measurable. Together these observations support the interpretation that electroporation can be repeatedly caused and observed in a viable tissue, without apparent damage.

We thank J. A. Jarrell and R. S. Langer, Jr. for helpful discussions.

This work supported partially by Ortho Diagnostic Systems, and by a National Science Foundation Fellowship to K. T. Powell.

Received for publication 30 September 1988 and in final form 31 May 1989.

REFERENCES

Abidor, I. G., V. B. Arakelyan, L. V. Chernomordik, Y. A. Chizmadzhev, V. F. Pastushenko, and M. R. Tarasevich. 1979. Electric breakdown of bilayer membranes. I. The main experimental facts and their qualitative significance. *Bioelectrochem. Bioenerg.* 6:37–52.

Benz, R., and F. Conti. 1981. Reversible electrical breakdown of squid giant axon membrane. *Biochim. Biophys. Acta.* 645:115–123.

Benz, R., and U. Zimmerman. 1980*a*. Relaxation studies on cell membranes and lipid bilayers in the high electric field range. *Bioelectrochem. Bioenerg.* 7:723–739.

Benz, R., and U. Zimmerman. 1980*b*. Pulse-length dependence of the electrical breakdown in lipid bilayer membranes. *Biochim. Biophys. Acta.* 597:637–642.

Benz, R., and U. Zimmerman. 1981. The resealing process of lipid bilayers after reversible electrical breakdown. *Biochim. Biophys. Acta.* 640:169–178.

Benz, R., F. Beckers, and U. Zimmerman. 1979. Reversible electrical breakdown of lipid bilayer membranes: a charge-pulse relaxation study. *J. Membr. Biol.* 48:181–204.

Berridge, M. J., and J. L. Oschman. 1972. Transporting Epithelia. Academic Press, Inc., New York. 24–25.

Candia, O. A. 1970. The hyperpolarization region of the current-voltage curve in frog skin. *Biophys. J.* 10:323–344.

Chernomordik, L. V., S. I. Sukharev, I. G. Abidor, and Y. A. Chizmadzhev. 1982. The study of the BLM reversible electrical breakdown mechanism in the presence of UO_2^{2+}. *Bioelectrochem. Bioenerg.* 9:149–155.

Chernomordik, L. V., S. I. Sukharev, I. G. Abidor, and Y. A. Chizmadzhev. 1983. Breakdown of lipid bilayer membranes in an electric field. *Biochim. Biophys. Acta.* 736:203–213.

Chernomordik, L. V., S. I. Sukharev, S. V. Popov, V. F. Pastushenko, A. V. Sokirko, I. G. Abidor, and Y. A. Chizmadzhev. 1987. The electrical breakdown of cell and lipid membranes: the similarity of phenomenologies. *Biochim. Biophys. Acta.* 902:360–373.

Coster, H. G. L., and U. Zimmerman. 1975. Dielectric breakdown in the membranes of *Valonia utricularis:* the role of energy dissipation. *Biochim. Biophys. Acta.* 382:410–418.

Crowley, J. M. 1973. Electrical breakdown of bimolecular lipid membranes as an electromechanical instability. *Biophys. J.* 13:711–724.

Finkelstein, A. 1964. Electrical excitability of isolated frog skin and toad bladder. *J. Gen. Physiol.* 47:545–565.

Geddes, L. A. 1972. Electrodes and the Measurement of Bioelectric Events. John Wiley & Sons, New York.

Glaser, R. W., S. L. Leikin, L. V. Chernomordik, V. F. Pastushenko, and A. I. Sokirko. 1988. Reversible electrical breakdown of lipid bilayers: formation and evolution of pores. *Biochim. Biophys. Acta.* 940:275–287.

Helman, S. I., and R. S. Fisher. 1977. Microelectrode studies of the active Na transport pathway of frog skin. *J. Gen. Physiol.* 69:571–604.

Helman, S. I., and D. A. Miller. 1971. In vitro techniques for avoiding edge damage in studies of frog skin. *Science (Wash. DC).* 173:146–148.

Kinosita, K., Jr., and T. Y. Tsong. 1977. Hemolysis of human erythrocytes by a transient electric field. *Proc. Natl. Acad. Sci. USA.* 74:1923–1927.

Lee, R. C., D. C. Gaylor, D. Bhatt, and D. A. Israel. 1988. Role of cell membrane rupture in the pathogenesis of electrical trauma. *J. Surg. Res.* 47:709–719.

Michel, M. R., M. Elgizoli, H. Koblet, and C. Kempf. 1988. Diffusion loading conditions determine recovery of protein synthesis in electroporated P3X63 Ag8 cells. *Experientia (Basel).* 44:199–203.

Neumann, E., A. Sowers, and C. Jordan, editors. 1989. Electroporation and Electrofusion in Cell Biology. Plenum Publishing Corp., New York.

Powell, K. T., E. G. Derrick, and J. C. Weaver. 1986. A quantitative theory of reversible electrical breakdown. *Bioelectrochem. Bioelectroenerg.* 15:243–255.

Stämpfi, R. 1958. Reversible electrical breakdown of the excitable membrane of a Ranvier node. *An. Acad. Bras. Cienc.* 30:57–63.

Sugar, I. P. 1981. The effects of external fields on the structure of lipid bilayers. *J. Physiol (Paris).* 77:1035–1042.

Sukharev, S. I., I. G. Abidor, and Y. A. Chizmadzhev. 1982. The study of the BLM reversible electrical breakdown mechanism in the presence of UO_2^{2+}. *Bioelectrochem. Bioenerg.* 9:149–155.

Weaver, J. C., and R. A. Mintzer. 1981. Decreased bilayer stability due to transmembrane potentials. *Phys. Lett.* 86A:57–59.

Weaver, J. C., and K. T. Powell. 1989. Theory of electroporation. *In* Electroporation and Electrofusion in Cell Biology. E. Neumann, A. Sowers, and C. Jordan, editors. Plenum Publishing Corp., New York. 111–126.

Weaver, J. C., G. I. Harrison, J. G. Bliss, J. R. Mourant, and K. T. Powell. 1988. Electroporation: high frequency of occurrence of the transient high permeability state in red blood cells and intact yeast. *FEBS (Fed. Eur. Biochem. Soc.) Lett.* 229:30–34.

Zimmerman, U. 1986. Electrical breakdown, electropermeabilization and electrofusion. *Rev. Physiol. Biochem. Pharmacol.* 105:175–256.

Zimmerman, U., J. Schultz, and G. Pilwat. 1973. Transcellular ion flow in *Escherichia coli* B and electrical sizing of bacterias. *Biophys. J.* 13:1005–1013.